Metal ion induced allosteric transition in the catalytic activity of an artificial phosphodiesterase†

Shinji Takebayashi,[a] Seiji Shinkai,*[a] Masato Ikeda[b] and Masayuki Takeuchi*[c]

Received 19th October 2007, Accepted 26th November 2007
First published as an Advance Article on the web 12th December 2007
DOI: 10.1039/b716196d

An artificial phosphodiesterase (**1**) bearing two types of metal binding sites, a catalytic site and a regulatory bipyridine site showed a unique allosteric transition in the catalytic activity against the metal concentration. The rate constants for the hydrolysis reaction of 2-hydroxypropyl-*p*-nitrophenyl phosphate (HPNP) and RNA dimer (ApA) with and without an effector metal ion were evaluated; the k_{obs} value of HPNP hydrolysis for **1**·$(Zn^{2+})_3$ (2.0×10^{-4} s^{-1}) is 3.3 times larger than that for **1**·$(Zn^{2+})_2$. In the case of **1** and Cu^{2+}, a 19.4 times larger k_{obs} value was obtained for **1**·$(Cu^{2+})_3$ (1.2×10^{-3} s^{-1}) against **1**·$(Cu^{2+})_2$. The increase in the catalytic activity is ascribed to the allosteric conformational transition of **1** induced by the coordination of effector metal ion to the Bpy moiety. A detailed investigation revealed that a conformational change of **1** induced by the third M^{2+} complexation enhances the rate of hydrolysis rather than a change in the substrate affinity.

Introduction

The design of artificial allosteric systems is of great significance for regulating the catalytic activities and complexation properties of artificial receptors.[1] We have been interested in the exploitation of homotropic allosteric systems, which show the nonlinear amplification of binding events and chemical signals.[2] This phenomenon is useful to control the activities of an artificial receptor in an OFF–ON switching manner at a threshold condition.[1,2] Allosteric molecular recognition systems have been studied well, whereas studies on artificial allosteric catalytic systems are still very rare.[3,4] Furthermore, as far as we know, there are few reports of the same metal ion playing both roles of a catalytic metal ion and an effector metal ion, giving rise to an allosteric transition phenomenon.[3–5] Such novel systems would show a unique catalytic activity response depending on the metal ion concentration.

There is considerable interest in creating artificial phosphodiesterases because of their potential application to gene therapy. For this purpose, numerous catalysts containing essential metal ions have been explored.[6] Recently, we designed compound **1** as an allosteric artificial phosphodiesterase, which has two different types of metal ion binding sites, 2,2′-bipyridine (Bpy) as a regulatory site and 2,2′-dipicolylamine (DPA) as catalytic sites (Fig. 1).[7]

The DPA moieties have higher Zn^{2+} or Cu^{2+} affinities than the Bpy moiety;[8] as a result, the first two metal ions are bound to two DPA moieties in **1** to produce **1**·$(M^{2+})_2$ ($M^{2+} = Zn^{2+}$ or Cu^{2+}). The regulatory Bpy moiety adopts mostly a transoid conformation because of the repulsion between lone-pairs of nitrogen atoms,[9] where the amine distance between DPA is estimated to be 0.84 nm by the molecular modeling (see Fig. 2: Insight II, Discover 3). The

[a]*Department of Chemistry and Biochemistry, Graduate School of Engineering, Kyushu University, Fukuoka, 819-0395, Japan. E-mail: seijitcm@mbox.nc.kyushu-u.ac.jp; Fax: (+81) 92 802 2818; Tel: (+81) 92 802 2820*
[b]*Department of Synthetic Chemistry and Biological Chemistry, Graduate School of Engineering, Kyoto University, Kyoto, 615-8510, Japan*
[c]*Macromolecules Group, Organic Nanomaterials Center, National Institute for Materials Science, Tsukuba, 305-0047, Japan. E-mail: TAKEUCHI.Masayuki@nims.go.jp; Fax: (+81) 29 859 2101; Tel: (+81) 29 859 2110*

† Electronic supplementary information (ESI) available: Fig. S1: ^{1}H NMR spectra (9.5–6.5 ppm) for **1** + $Zn(ClO_4)_2$. Fig. S2: ^{1}H NMR spectra (6.0–3.0 ppm) for **1** + $Zn(ClO_4)_2$. Fig. S3: ESI MS spectra for $[Zn^{2+}]/[\mathbf{1}] = 2.0$ and 8.0 and $[Cu^{2+}]/[\mathbf{1}] = 2.0$ and 3.0 in 33% ethanol–water (HEPES, 25 mM). Fig. S4: Lineweaver–Burk plots for HPNP cleavage. Fig. S5: UV-Vis spectral changes of **1**·$(Zn^{2+})_3$ upon addition of EDTA-2Na in 33% ethanol–water (HEPES, 25 mM). See DOI: 10.1039/b716196d

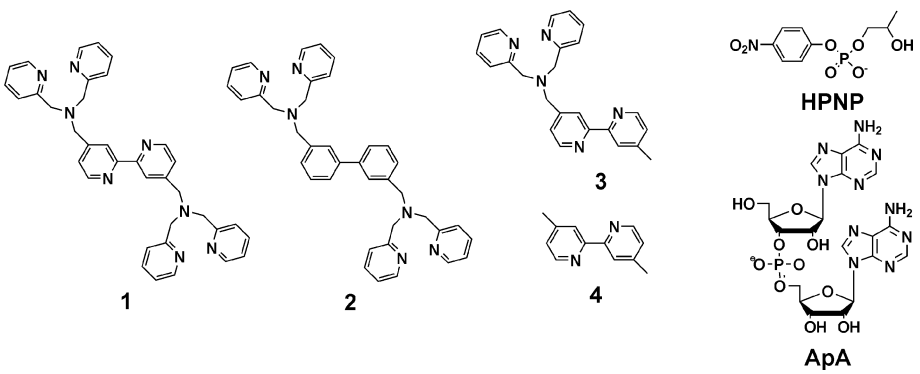

Fig. 1 Chemical structures of compounds **1–4** and substrates HPNP and ApA.

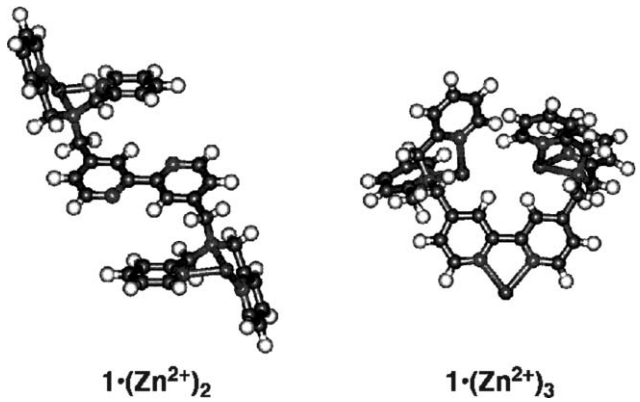

Fig. 2 The molecular models of **1**·$(Zn^{2+})_2$ and **1**·$(Zn^{2+})_3$.

metal ion coordination to Bpy results in a conformational change from transoid to cisoid by enforcing an alignment of the DPA sites at a distance of 0.48 nm (catalytically more active); that is an allosteric transition. Compounds **2–4** used for control experiments cannot show such an allosteric transition phenomenon.

We demonstrated preliminary results on an allosteric transition of **1** in the recent communication,[7] wherein **1** can alter its catalytic activity upon addition of metal ions (Zn^{2+} or Cu^{2+}) in the hydrolysis of 2-hydroxypropyl-*p*-nitrophenyl phosphate (HPNP). This preliminary finding stimulated us to further investigate in detail the influence of the metal binding on the catalytic hydrolysis reaction of HPNP. In this publication, we report the investigations of the metal-induced allosteric transition in the catalytic activity of **1** and further demonstrated the allosteric catalysis for RNA dinucleotide, ApA, as a substrate.

Results and discussion

Synthesis of compounds 1–3

The synthetic pathways for compounds **1–3** are shown in Schemes 1, 2, 3. Compound **1** was synthesized by reductive amination of 2,2′-bipyridine-4,4′-dicarbaldehyde with 2,2′-dipicolylamine. We selected sodium triacetoxyborohydride [$NaBH(OAc)_3$] as a reducing agent (Scheme 1).[10] The methyl groups of 3,3′-dimethylbiphenyl were brominated with 1,3-dibromo-5,5′-dimethylhydantoin (BDH) in carbon tetrachloride in the presence of benzoyl peroxide to give 3,3′-dibromomethylbiphenyl (**5**) (Scheme 2).[11] Compound **4** was reacted with lithium diisopropylaminde, and the anion thus formed was trapped with trimethylsilyl chloride (TMSCl) to generate 4-trimethylsilyl-4′-methyl-2,2′-bipyridine (**6**) (Scheme 3).[12] The TMS group of **6** was removed using dry fluoride anion sources (CsF in DMF) in the presence of BrF_2CCF_2Br to produce the 4-bromomethyl-4′-methyl-2,2′-bipyridine (**7**). Compounds **2** and **3** were synthesized from the corresponding bromomethyl precursors **5** and **7** by the nucleophilic substitution with 2,2′-dipicolylamine.

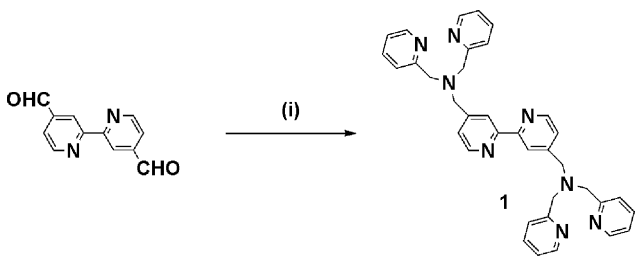

Scheme 1 Synthesis of **1**. *Reagents and conditions*: (i) 2,2′-dipicolylamine, $NaBH(OAc)_3$, $ClCH_2CH_2Cl$, r.t., 18 h.

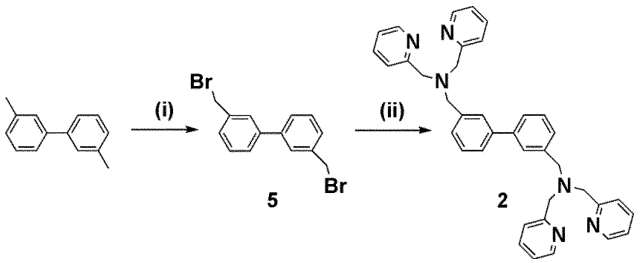

Scheme 2 Synthesis of **2**. *Reagents and conditions*: (i) BDH, benzyl peroxide, dry CCl_4, reflux, 4 h; (ii) 2,2′-dipicolylamine, KI, K_2CO_3, dry CH_3CN, 35 °C, 5 h.

In situ sequential formation of trinuclear metal complex of 1

The complexation behaviour of **1** with Zn^{2+} and Cu^{2+} (as perchlorate salts) in ethanol–water (HEPES, 16 mM) = 1/2 (v/v) solution at pH 7.7 and 25 °C was monitored by photometric titration, ESI MS and ^1H NMR spectroscopies.

Binding processes of Zn^{2+} to **1** (0.40 mM) were accompanied by three steps of spectral changes with isosbestic points observed at 293.2 nm (0 to 1 equiv. Zn^{2+}), 296.8 nm (1 to 2 equiv. Zn^{2+}) and 297.4 nm (more than 2 equiv. Zn^{2+}) (Fig. 3(a)). The absorbance of DPA moieties changed almost linearly upon addition of 0 to 1 equiv. Zn^{2+} and 1 to 2 equiv. Zn^{2+}. This result clearly showed that two Zn^{2+} ions are bound firstly to the DPA moieties quantitatively to produce **1**·$(Zn^{2+})_2$ under these conditions. At [Zn^{2+}] higher than 2 equiv., a typical shift from 284.6 to 312.0 nm in the absorption band of the Bpy moiety was observed; Bpy·Zn^{2+} is formed at this stage (Fig. 4). A plot of the absorbance at 312.0 nm against Zn^{2+} concentration showed a saturation behaviour and the association constant for the formation of **1**·$(Zn^{2+})_3$ from **1**·$(Zn^{2+})_2$ was evaluated to be 9.1×10^2 M^{-1}. Similar results were obtained

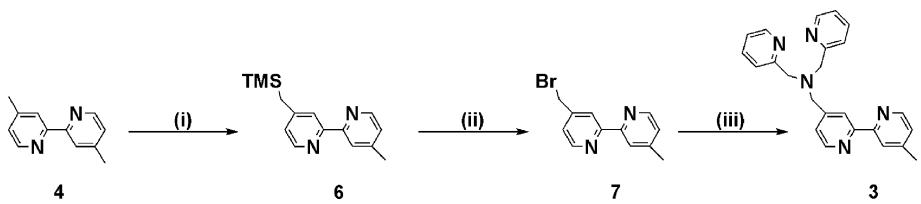

Scheme 3 Synthesis of **3**. *Reagents and conditions*: (i) LDA/THF, TMSCl, dry THF, 0 °C, 30 min; (ii) CsF, BrF_2CCF_2Br, dry DMF, r.t., 2 h; (iii) 2,2′-dipicolylamine, K_2CO_3, KI, dry CH_3CN, 35 °C, 2 h.

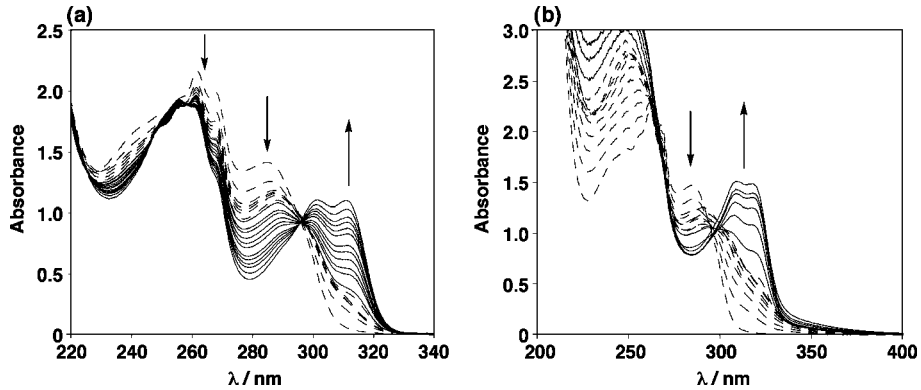

Fig. 3 (a) UV-Vis spectral changes of **1** (0.4 mM) upon addition of $Zn(ClO_4)_2$ (broken lines; 0–2 equiv., solid lines; 2–11 equiv.) in 33% ethanol–water (HEPES, 25 mM) at pH 7.7 and 25 °C, (b) UV-Vis spectral changes of **1** (1.0 mM) upon addition of $Cu(ClO_4)_2$ (broken lines; 0–2 equiv., solid lines; 2–6 equiv.) in 33% ethanol–water (HEPES, 25 mM) at pH 7.7 and 25 °C.

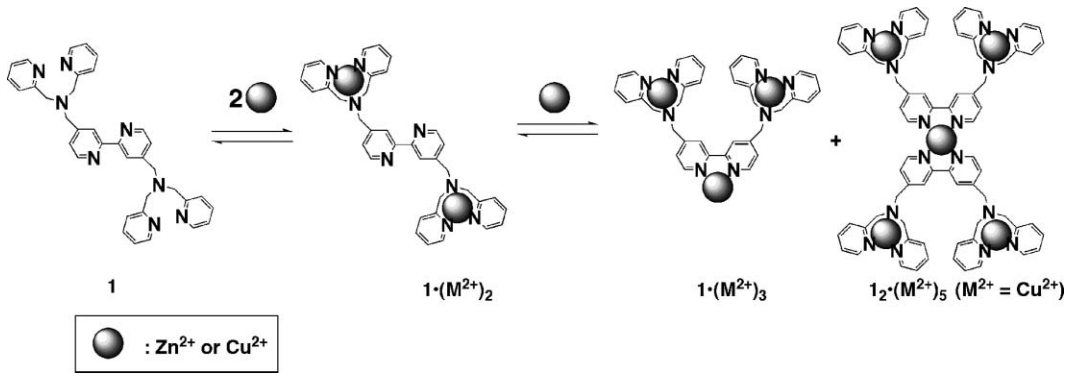

Fig. 4 Schematic representation for the sequential complexation of metal ions to **1**.

for the **1** (1.0 mM) and Cu^{2+} system, where 2 equiv. of Cu^{2+} were bound to the DPA moieties in **1** quantitatively (Fig. 3(b)). The association constants for the formation of $\mathbf{1}\cdot(Cu^{2+})_3$ and $\mathbf{1}_2\cdot(Cu^{2+})_5$ from $\mathbf{1}\cdot(Cu^{2+})_2$ were evaluated to be 6.3×10^4 M^{-1} and 1.0×10^8 M^{-2}, respectively (Fig. 4).

^{1}H NMR titration experiments (see supplementary information†) also supported this sequential binding scheme shown in Fig. 4. The *in situ* formation of $\mathbf{1}\cdot(M^{2+})_3$ and $\mathbf{1}_2\cdot(M^{2+})_5$ (for Cu^{2+}) from $\mathbf{1}\cdot(M^{2+})_2$ was further supported by the ESI MS measurement. The ESI MS spectra for $[Zn^{2+}]/[\mathbf{1}] = 2.0$, 8.0 in 33% ethanol–water (HEPES, 25 mM) showed strong peaks at $m/z = 1007.1$ and 1271.0, which are assignable to the species of $[1\cdot(Zn^{2+})_2\cdot(ClO_4^-)_3]^+$ (calc. for $[1\cdot(Zn^{2+})_2\cdot(ClO_4^-)_3]^+ = 1007.0$) and $[1\cdot(Zn^{2+})_3\cdot(ClO_4^-)_5]^+$ (calc. for $[1\cdot(Zn^{2+})_2\cdot(ClO_4^-)_3]^+ = 1270.8$), respectively (see supplementary data,† Fig. S3(a) and (b)). The ESI MS spectrum for $[Cu^{2+}]/[\mathbf{1}] = 2.0$, 3.0 in 33% ethanol–water (HEPES, 25 mM) showed strong peaks at $m/z = 1003.1$ and 1266.0, which are assignable to the species of $[1\cdot(Cu^{2+})_2\cdot(ClO_4^-)_3]^+$ (calc. for $[1\cdot(Cu^{2+})_2\cdot(ClO_4^-)_3]^+ = 1003.0$) and $[1\cdot(Cu^{2+})_3\cdot(ClO_4^-)_5]^+$ (calc. for $[1\cdot(Cu^{2+})_2\cdot(ClO_4^-)_3]^+ = 1265.8$), respectively (see supplementary data,† Fig. S3(c) and (d)).

Hydrolysis of HPNP by Zn(II) and Cu(II) complexes of 1

We firstly employed HPNP as a substrate. Kinetic experiments were conducted on the basis of the release rate of *p*-nitrophenolate from HPNP by monitoring the increase in the absorbance at 406 nm. The kinetic studies at varying pH were performed and pseudo-first-order-rate constants (k_{obs}) were evaluated for $\mathbf{1}\cdot(Zn^{2+})_3$. The pH-rate profile for the transesterification of HPNP catalyzed by $\mathbf{1}\cdot(Zn^{2+})_3$ is bell-shaped in the pH region 6.0–8.0 with a maximum at pH 7.7 (Fig. 5). A bell-shaped pH rate profile is often observed for metal-promoted HPNP cleavage. This bell-type curve indicates that cooperativity between the metal centers in DPA would be due to the occurrence of general-acid/general-base

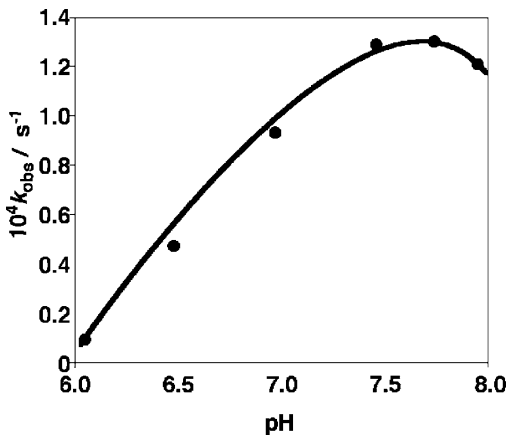

Fig. 5 Effect of pH on the observed rate constants measured for the cleavage of HPNP by $\mathbf{1}\cdot(Zn^{2+})_3$. *Reagents and conditions*: [**1**] = 0.40 mM, $[Zn(ClO_4)_2] = 2.0$ mM, [HPNP] = 0.80 mM.

catalysis. The increase in the rate with increasing pH is explained by generation of metal-promoted hydroxide, which acts as a general base in HPNP cleavage. The decrease in the rate at higher pH might reflect the competitive binding of hydroxide to the catalyst which prevents binding of the substrate.

Then, the kinetic studies at varying Zn^{2+} to Cu^{2+} concentrations were performed and pseudo-first-order rate constants (k_{obs}) were evaluated for **1** and **2** (Fig. 6). Very interestingly, in the case of **1**, there was a further significant increase in the catalytic activity upon addition of more than 2 equiv. metal ion, whereas such enhancement was not observed for **2** without the regulatory site (Fig. 6). In Fig. 6(a), the rate constant for **1** with 8 equiv. Zn^{2+} is 3.3 times larger than for **1** with 2 equiv. Zn^{2+} (**1**·$(Zn^{2+})_2$). The saturation behaviour observed for **1** in Fig. 6(a) is complementary to the results of photometric titration. In the case of **1** and Cu^{2+}, 19.4 times larger k_{obs} value was obtained for **1** with 3 equiv. Cu^{2+} against **1** with 2 equiv. Cu^{2+}(**1**$(Cu^{2+})_2$) (Fig. 6(b)). For **1** with 3 equiv. Cu^{2+}, the ratio of [**1**·$(Cu^{2+})_3$]/[$\mathbf{1}_2$·$(Cu^{2+})_5$]/[**1**·$(Cu^{2+})_2$] is estimated to be 81/11/8 by the association constants between Cu^{2+} and the Bpy moiety in **1**.[13] These results clearly show that **1**·$(M^{2+})_3$ and/or $\mathbf{1}_2$·$(M^{2+})_5$ have higher catalytic activity than **1**·$(M^{2+})_2$.

In order to evaluate the contribution of the Bpy·Zn^{2+} complex to the hydrolysis of HPNP, k_{obs} values with control compounds **3** and **4** were measured. It was found that k_{obs} value of 6.6×10^{-5} s^{-1} obtained from a mixture of **2**·$(Zn^{2+})_2$ and **4**·Zn^{2+} is almost same as that obtained from **2**·$(Zn^{2+})_2$ (6.2×10^{-5} s^{-1}). In addition, the k_{obs} value of 3.5×10^{-5} s^{-1} for **3**·$(Zn^{2+})_2$ is 5.8 times smaller than that for **1**·$(Zn^{2+})_3$. These results show that inter- or intra-molecular reaction catalyzed by Bpy·Zn^{2+} and DPA·Zn^{2+} complexes is not effective for the hydrolysis of HPNP (Table 1(a)–(d)). Similar results were obtained from Cu^{2+} (Table 1(e)–(h)). The k_{obs} value of 1.2×10^{-3} s^{-1} for **1**·$(Cu^{2+})_3$ + $\mathbf{1}_2$·$(Cu^{2+})_5$ is 40 times larger than that for other control complexes. The increase in the catalytic activity is ascribed, therefore, to the allosteric conformational transition of **1** induced by the coordination of effector metal ion to the Bpy moiety as shown in Fig. 4.

Michaelis–Menten kinetic parameters were evaluated from saturation kinetic experiments to obtain a further insight into the rate enhancement observed for **1**. Saturation kinetic curves were obtained from Zn^{2+} and Cu^{2+} catalysts. A Lineweaver–Burk plot was applied to calculate the Michaelis–Menten constant (K_m) and the catalytic constant (k_{cat}) (see supplementary information†). The results are summarized in Table 1. A significant increase in the value of k_{cat} (4.1 times for Zn^{2+} and 55 times for Cu^{2+}) was obtained from the conditions (b) and (d) compared with (a) and (c) in Table 2. A conformational change of **1** induced by the third M^{2+} complexation, that is, allosteric transition, enhanced the rate of hydrolysis but not by a change in the substrate affinity. This should be a consequence of the preferable preorganization of two DPA·M^{2+} complex units toward the hydrolysis; the conformational change of this catalyst would facilitate the attack of intramolecular hydroxyl ion sitting on M^{2+} to the substrate.

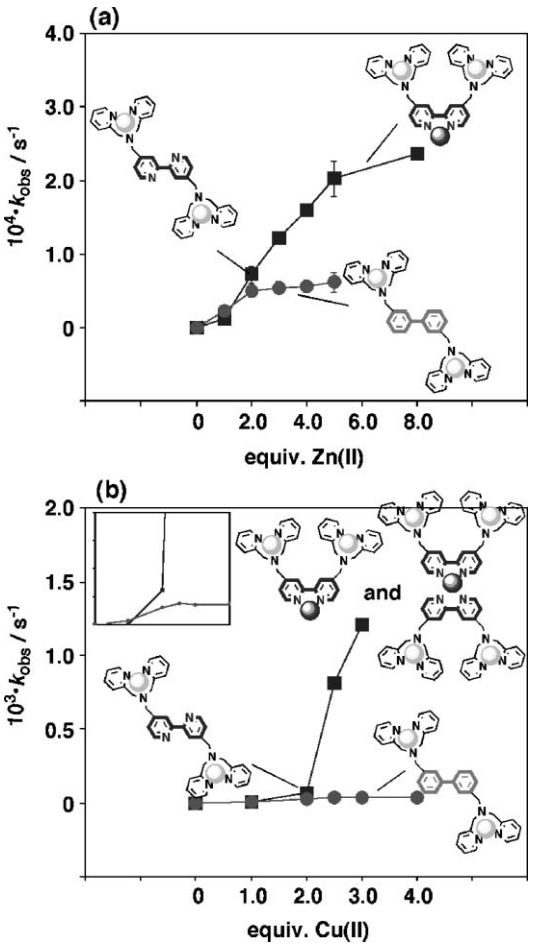

Fig. 6 (a) Plots of pseudo-first-order rate constants (k_{obs}) for the hydrolysis of HPNP (0.80 mM) at various Zn^{2+} concentrations in 33% ethanol–water (HEPES, 25 mM): (a) [**1**] = 0.40 mM (■), [**2**] = 0.40 mM (●) pH 7.7 at 25 °C. (b) Plots of pseudo-first-order rate constants (k_{obs}) for the hydrolysis of HPNP (1.0 mM) at various Cu^{2+} concentrations in 33% ethanol–water (HEPES, 25 mM): (a) [**1**] = 1.0 mM (■), [**2**] = 1.0 mM (●) pH 7.7 at 25 °C. Inset is an enlarged view for **2** and Cu^{2+}.

Table 1 Pseudo-first-order rate constants (k_{obs}) for the hydrolysis of HPNP Zn(II) and Cu(II) complexes of **1–4**[a]

	$10^3 k_{obs}/s^{-1}$
(a) **1** (0.40 mM) with $Zn(ClO_4)_2$ (2.0 mM)[b]	0.20
(b) **2** (0.40 mM) with $Zn(ClO_4)_2$ (2.0 mM)[b]	0.062
(c) **2** (0.40 mM) + **4** (0.40 mM) with $Zn(ClO_4)_2$ (2.0 mM)[b]	0.066
(d) **3** (0.40 mM) with $Zn(ClO_4)_2$ (2.0 mM)[b]	0.035
(e) **1** (1.0 mM) with $Cu(ClO_4)_2$ (3.0 mM)[c]	1.2
(f) **2** (1.0 mM) with $Cu(ClO_4)_2$ (2.0 mM)[c]	0.030
(g) **2** (1.0 mM) + **4** (1.0 mM) with $Cu(ClO_4)_2$ (3.0 mM)[c]	0.028
(h) **3** (1.0 mM) with $Cu(ClO_4)_2$ (2.0 mM)[c]	0.032

[a] In 33% ethanol–water (HEPES, 25 mM), pH 7.7 at 25 °C. [b] [HPNP] = 0.8 mM. [c] [HPNP] = 1.0 mM

Table 2 Michaelis–Menten kinetic parameters estimated by Lineweaver–Burk plots for HPNP cleavage; in ethanol–water (HEPES, 25 mM), pH 7.7 at 25 °C

	$10^3 k_{cat}/s^{-1}$	$10^3 K_m/M$
(a) **1** (0.40 mM) with $Zn(ClO_4)_2$ (0.8 mM)	0.51	1.93
(b) **1** (0.40 mM) with $Zn(ClO_4)_2$ (2.0 mM)	2.10	3.13
(c) **1** (1.0 mM) with $Cu(ClO_4)_2$ (2.0 mM)	0.26	3.56
(d) **1** (1.0 mM) with $Cu(ClO_4)_2$ (3.0 mM)	14.3	12.7

Upon addition and removal of the third metal ion bound to BPy, we confirmed the conversion between $\mathbf{1}\cdot(M^{2+})_3$ and $\mathbf{1}\cdot(M^{2+})_2$ by UV-vis spectroscopic method (supplementary information†); this indicates that the ON–OFF experiments using this system can be demonstrated. At first, HPNP was added to a solution of $\mathbf{1}\cdot(M^{2+})_2$. Absorbance at 406 nm assignable to *p*-nitrophenolate slowly increased. After 3 min, the addition of metal ion to the reaction mixtures caused a sharp increase in the formation of *p*-nitrophenolate. Next, the removal of metal ion by the addition of EDTA resulted in the decrease in the rate of hydrolysis again (Fig. 7). The results further support the view that the third metal ion acts as an allosteric effector for this hydrolysis reaction.

Hydrolysis of ApA by Zn(II) and Cu(II) complexes

With such an outstanding catalyst in hands we turned to more appealing substrates such as RNA dinucleotides; namely ApA. The cleavage process was followed by HPLC, monitoring the disappearance of the substrate and the formation 3′-AMP and adenosine. The k_{obs} values were calculated from changes in these species (Table 3). We set the reaction temperature at 35 °C for Zn^{2+} complex and 45 °C for Cu^{2+} complex because the reaction was not sufficiently fast for monitoring at 25 °C. We confirmed that the metal binding process are almost the same as those observed at 25 °C. The k_{obs} value of 3.6×10^{-4} s^{-1} for $\mathbf{1}\cdot(Zn^{2+})_3$ was 33 times larger than that for $\mathbf{1}\cdot(Zn^{2+})_2$ ($k_{obs} = 1.1 \times 10^{-5}$ s^{-1}). In the case of Cu^{2+} system, the hydrolysis reaction with $\mathbf{1}\cdot(Cu^{2+})_2$ was too slow to follow. On the contrary, k_{obs} for $\mathbf{1}\cdot(Cu^{2+})_3$ was evaluated to be 1.4×10^{-5} s^{-1}, which is consistent with the data demonstrated by other groups.[6] These results clearly show that $\mathbf{1}\cdot(M^{2+})_n$ can also alter their catalytic activities in the hydrolysis reaction of ApA.

Table 3 Pseudo-first-order rate constants (k_{obs}) for the hydrolysis of ApA by Zn(II) and Cu(II) complexes of **1**[a]

	$10^4 k_{obs}/s^{-1}$
1 with 2 equiv. Zn^{2+} [b]	0.11
1 with 8 equiv. Zn^{2+} [b]	3.6
1 with 2 equiv. Cu^{2+} [c]	—[d]
1 with 3 equiv. Cu^{2+} [c]	1.4

[a] In 37% ethanol–water (HEPES, 25 mM), pH 7.7, [ApA] = 0.10 mM. [b] [**1**] = 1.0 mM, [$Zn(ClO_4)_2$] = 2.0, 8.0 mM, at 35 °C. [c] [**1**] = 1.0 mM, [$Cu(ClO_4)_2$] = 2.0, 3.0 mM, at 45 °C. [d] The rate was too slow to evaluate.

Conclusions

In conclusion, we have demonstrated that compound **1** bearing two types of Zn^{2+} or Cu^{2+} binding sites exhibits an allosteric response in the catalytic activities toward the hydrolysis of phosphodiester substrates such as HPNP and ApA. We anticipate, therefore, that such a supramolecular catalytic system would further produce intelligent artificial systems responding to various types of chemical stimuli.

Experimental

^{1}H NMR, absorption spectra, MALDI TOF MS, ESI MS spectra were measured with Bruker DMX 600, Shimadzu UV-2500, Perseptive Voyager RP MALDI TOF spectrometer, Perseptive Mariner and JASCO J-720 WI, respectively.

For the cleavage of ApA the reaction was followed by HPLC by withdrawing 10 μl of the mixture from 100 μl of the reaction solution and 100 μl of mobile phase condition A (see below). Separation condition: column C30-UG-5 (4.6 nm, 250 nm); mobile phase (condition A = 10 mM NaH_2PO_4, 10 mM Sodium octanesulfonate, 5 mM EDTA-2Na); eluent gradient with acetonitrile (A: 100 - 80% (0–8.0 min), 80–20% (8.0–8.1 min), 30% (8.1–25.0 min.), 30–100% (25.0–25.1 min), and 100% (25.1–30 min)); flow rate 1.0 ml min^{-1}; temperature 40 °C; detection wavelength 254 nm.

Syntheses

4,4′-Dimethyl-2,2′-bipyridine **4**[14] and HPNP[15] were synthesized according to the previously reported methods. ^{1}H NMR, absorption spectra, MALDI TOF MS, ESI MS spectra were measured with Bruker DMX 600, Shimadzu UV-2500, Perseptive Voyager RP MALDI TOF spectrometer, Perseptive Mariner and JASCO J-720 WI, respectively.

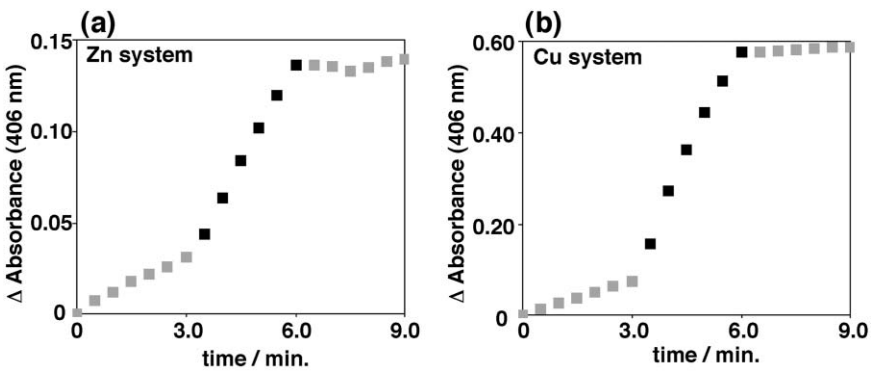

Fig. 7 Control of hydrolysis for HPNP upon addition and removal of allosteric metal ion: (a) [**1**] = 0.40 mM, [$Zn(ClO_4)_2$] = 2.0 mM, [HPNP] = 1.0 mM (0 min), addition of $Zn(ClO_4)_2$ (3.0 mM) after 3 min, and addition of EDTA (3.0 mM) after 6 min in ethanol–water (HEPES, 25 mM), pH 7.7 at 25 °C.

4,4′-Bis(dipicolylaminomethyl)-2,2′-bipyridine (1)

4,4′-Diformyl-2,2′-bipyridine (200 mg, 0.94 mmol) and 2,2′-dipicolylamine (0.34 ml, 1.9 mmol) were dissolved in 30 ml of dichloroethane. To this solution sodium triacetoxyborohydride (540 mg, 2.5 mmol) was added and the resultant mixture was stirred at room temperature for 18 h. After addition of 5% aqueous NH_3, the insoluble material was filtered off. The filtrate was concentrated *in vacuo*. The residual aqueous solution was extracted by chloroform and dried over anhydrous sodium sulfate. The solution was evaporated to dryness, the oil residue being chromatographed (silica gel, chloroform–methanol = 50 : 1 with four drops of 28% aqueous NH_3) to give yellow solid. The resultant yellow solid was washed by ether to give **1** as a white powder (253 mg, 46%); mp 135.9–137.9 °C. ^{1}H NMR (600 MHz, $CDCl_3$, 27 °C, δ/ppm, J/Hz): 3.81 (s, 4H), 3.85 (s, 8H), 7.15 (t, J = 6.0, 4H), 7.47 (d, J = 4.8, 2H), 7.59 (d, J = 7.7, 4H), 7.67 (t, J = 7.5, 4H), 8.38 (s, 2H), 8.53 (d, J = 4.5, 4H), 8.63 (d, J = 4.9, 2H); MALDI TOF MS (dithranol matrix): calc. (found) for [**1** + H]$^+$: 579.71 (579.71). Calc. for $C_{36}H_{34}N_8 \cdot 0.5CH_3OH$: C, 73.71; H, 6.10; N, 18.84. Found: C, 73.50; H, 5.93; N, 18.77%.

3,3′-Dibromomethylbiphenyl (5)

To a solution of 3,3′-dimethylbiphenyl (0.5 ml, 2.54 mmol) with dry CCl_4 (30 ml) were added BDH (940 mg, 3.30 mmol) and BPO (108 mg, 0.48 mmol). The mixture was allowed to reflux under N_2 for 4 h. The resultant precipitate was filtered off and the filtrate was evaporated under reduced pressure. The residue was recrystallized from hexane and chloroform to afford the product as a white solid (200 mg, 22%). ^{1}H NMR (250 MHz, $CDCl_3$, 27 °C, δ/ppm, J/Hz): 4.56 (s, 4H), 7.46 (m, 6H), 7.61 (s, 2H).

3,3′-Bis(dipicolylaminomethyl)biphenyl (2)

To a solution of 3,3′-dibromomethylbiphenyl **5** (195 mg, 0.57 mmol) with dry acetonitrile (10 ml) were added K_2CO_3 (400 mg, 2.89 mmol), KI (38 mg, 0.23 mmol) and dipicolylamine (0.20 ml, 1.1 mmol). The mixture was allowed to stir at 35 °C under N_2 for 5 h. The resultant precipitate was filtered off and the filtrate was evaporated under reduced pressure. The residue was dissolved in chloroform and washed with aqueous Na_2CO_3 (2 × 20 ml). The organic extract was dried over anhydrous Na_2SO_4. After removal of solvent under reduced pressure, the residue was purified by column chromatography (silica gel, chloroform–methanol = 25 : 1 (v/v) saturated 28% aqueous ammonia) to give yellow oil compound **2** (158 mg, 48%). ^{1}H NMR (600 MHz, $CDCl_3$, 27 °C, δ/ppm, J/Hz) 3.77 (s, 4H), 3.86 (s, 8H), 7.14 (t, J = 5.9, 4H), 7.42 (m, 6H), 7.63 (m, 10H), 8.52 (d, J = 4.7, 4H); MALDI TOF MS (dithranol matrix): calc. (found) for [**2** + H]$^+$: 577.73 (577.40). Calc. for $C_{38}H_{36}N_6 \cdot 1.0CHCl_3$: C, 67.29; H, 5.36; N, 12.07. Found: C, 67.35; H, 5.48; N, 12.00%.

4-Trimethylsilyl-4′-methyl-2,2′-bipyridine (6)

To a solution of 4,4′-dimethyl-2,2′-bipyridine (500 mg, 2.7 mmol) with dry THF (25 ml) was added dropwise 0.24 M LDA (11.4 ml, 2.7 mmol) with stirring under N_2 for 30 min at 0 °C. To the mixture was added dropwise TMSCl (0.5 ml, 3.0 mmol), and the reaction was stopped by addition of EtOH (1.0 ml). To the resultant mixture was added saturated aqueous $NaHCO_3$ (50 ml), and the product was extracted with ethyl acetate (3 × 30 ml). The organic extract was washed with brine (3 × 30 ml). The organic extract was dried over Na_2CO_3, filtered, and concentrated to give crude **5** (408 mg, 28% calculated by ^{1}H NMR spectrum). The residue was subjected to the next step without further purification.

4-Bromomethyl-4′-methyl-2,2′-bipyridine (7)

To a solution of crude **6** (312 mg, 0.58 mmol calculated by ^{1}H NMR spectrum) with dry DMF (10 ml) were added 1,2-dibromo-1,1,2,2-tetrafluoroethane (0.14 ml, 1.16 mmol) and CsF (0.2 g, 1.3 mmol) with stirring under N_2 at room temperature for 2 hours. The resultant precipitate was filtered off. To the filtrate was added water (50 ml), and the product was extracted with ethyl acetate (3 × 30 ml). The organic extract was washed with brine and water (3 × 30 ml, respectively). The organic extract was dried over Na_2CO_3, filtered, and concentrated to give crude **6** (269 mg, 35% calculated by ^{1}H NMR spectrum). The residue was subjected to the next step without further purification.

4-Dipicolylaminomethyl-4′-methyl-2,2′-bipyridine (3)

To a solution of crude **7** (269 mg, 0.20 mmol calculated by ^{1}H-NMR spectrum) with dry DMF (3 ml) and dry acetonitrile (7 ml) were added K_2CO_3 (83 mg, 0.60 mmol), KI (10 mg, 0.06 mmol) and dipicolylamine (0.04 ml, 0.22 mmol) with stirring under N_2 at 35 °C for 2 hours. The resultant precipitate was filtered off. The filtrate was washed with brine (3 × 30 ml), and the organic extract was dried over Na_2CO_3, filtered, and concentrated. The residue was purified by column chromatography (silica gel, chloroform–methanol = 30 : 1 (v/v) saturated 28% aqueous ammonia) to give yellow oily compound **3** (100 mg, 100%). ^{1}H NMR (600 MHz, $CDCl_3$, 27 °C, δ/ppm, J/Hz) 2.43 (s, 3H), 3.81 (s, 2H), 3.85 (s, 4H), 7.15 (m, 3H), 7.46 (d, J = 4.8, 1H), 7.59 (d, J = 7.8, 2H), 7.66 (t, J = 7.6, 2H), 8.20 (s, 1H), 8.38 (s, 1H), 8.53 (m, 3H), 8.63 (s, 1H); MALDI TOF MS (CHCA matrix): calc. (found) for [**3** + H]$^+$: 382.20 (382.24). Calc. for $C_{24}H_{23}N_5 \cdot 0.25CHCl_3$: C, 70.81; H, 5.70; N, 17.03. Found: C, 70.93; H, 5.88; N, 16.81%.

Acknowledgements

This study was supported partially by a Grant-in-Aid for Scientific Research B (17350071) (to M. T.) of the Ministry of Education, Culture, Science, Sports, and Technology (Japan). We thank Prof. Itaru Hamachi, Prof. Akio Ojida and Dr Masa-aki Inoue for helpful discussions. M. T. and S. T. thank Prof. Fumito Tani and Mr Jun Hagiwara for ESI MS measurements. S. T. thanks JSPS for the Research Fellowship for Young Scientists for financial support.

References

1 (*a*) For recent reviews on molecular switches and artificial allosteric systems: Special issue on molecular machines, *Acc. Chem. Res.*, 2001, **34**, no. 6); (*b*) J. Rebek, Jr., *Acc. Chem. Res.*, 1984, **17**, 258; (*c*) T. Nabeshima, *Coord. Chem. Rev.*, 1996, **148**, 151; (*d*) V. Balzani, M. Venturi and A. Credi, *Molecular Devices and Machines*, Wiley-VCH, Weinheim, 2003; (*e*) L. Kovbasyuk and R. Krämer, *Chem. Rev.*, 2004, **104**, 3161; (*f*) E. R. Kay, D. A. Leigh and F. Zerbetto, *Angew. Chem., Int. Ed.*, 2006, **46**, 72.

2 (*a*) S. Shinkai, M. Ikeda, A. Sugasaki and M. Takeuchi, *Acc. Chem. Res.*, 2001, **34**, 494; (*b*) M. Takeuchi, M. Ikeda, A. Sugasaki and S.

Shinkai, *Acc. Chem. Res.*, 2001, **34**, 865; (*c*) M. Ikeda, M. Takeuchi and S. Shinkai, *J. Synth. Org. Chem. Jpn.*, 2002, **60**, 1201.
3 (*a*) T. Tozawa, S. Tokiwa and Y. Kubo, *Tetrahedron Lett.*, 2002, **43**, 3455; (*b*) N. C. Gianneschi, P. A. Bertin, S. T. Nguyen, C. A. Mirkin, L. N. Zakharov and A. L. Rheingold, *J. Am. Chem. Soc.*, 2003, **125**, 10508; (*c*) N. C. Gianneschi, S.-H. Cho, S. T. Nguyen and C. A. Mirkin, *Angew. Chem., Int. Ed.*, 2004, **43**, 5503; (*d*) N. C. Gianneschi, S. T. Nguyen and C. A. Mirkin, *J. Am. Chem. Soc.*, 2005, **127**, 1644; (*e*) C. G. Oliveri, N. C. Gianneschi, S. T. Nguyen, C. A. Mirkin, C. L. Stern, Z. Wawrzak and M. Pink, *J. Am. Chem. Soc.*, 2006, **126**, 16286; (*f*) J. Kuwabara, C. L. Stern and C. A. Mirkin, *J. Am. Chem. Soc.*, 2007, **127**, 10074; (*g*) M. S. Masar III, N. C. Gianneschi, C. G. Oliveri, C. L. Stern, S. T. Nguyen and C. A. Mirkin, *J. Am. Chem. Soc.*, 2007, **127**, 10149; (*h*) H. J. Yoon, J. Heo and C. A. Mirkin, *J. Am. Chem. Soc.*, 2007, **127**, 14182.
4 (*a*) Krämer *et al.* and Scrimin *et al.* reported artificial allosteric catalysts, where ligands bound regulatory metal ions in advance: I. O. Fritsky, R. Ott, H. Pritzkow and R. Krämer, *Chem.–Eur. J.*, 2001, **7**, 122; (*b*) L. Kovbasyuk, H. Pritskow, R. Krämer and I. O. Fritsky, *Chem. Commun.*, 2004, 880; (*c*) A. Scarso, U. Scheffer, M. Göbel, Q. B. Broxterman, B. Kaptein, F. Formaggio, C. Toniolo and P. Scrimin, *Proc. Natl. Acad. Sci. U. S. A.*, 2002, **99**, 5144; (*d*) P. Scrimin, P. Tecilla, U. Tonellato, A. Veronese, M. Crisma, F. Formaggio and C. Toniolo, *Chem.–Eur. J.*, 2002, **8**, 2753; (*e*) A. Scarso, G. Zaupa, F. B. Houillon, L. J. Prins and P. Scrimin, *J. Org. Chem.*, 2007, **72**, 376.
5 Significant rate enhancement was observed for trinuclear Zn^{2+} complex (as a catalytic metal ion) for the hydrolysis of diribonucleotides: see ref. 6*b*.
6 (*a*) P. Molenveld, J. F. J. Engbersen and D. N. Reinhoudt, *Chem. Soc. Rev.*, 2000, **29**, 75; (*b*) M. Yashiro, A. Ishikubo and M. Komiyama, *Chem. Commun.*, 1997, 83; (*c*) J. Chin, *Curr. Opin. Chem. Biol.*, 1997, **1**, 514; (*d*) E. Kimura, S. Aoki, T. Koike and M. Shiro, *J. Am. Chem. Soc.*, 1997, **119**, 3068; (*e*) M. Arca, A. Bencini, E. Berni, C. Caltagirone, F. A. Devillanova, F. Isaia, A. Garau, C. Giorgi, V. Lippolis, A. Perra, L. Tei and B. Valtancoli, *Inorg. Chem.*, 2003, **42**, 6929; (*f*) H. A. Haddou, J. Sumaoka, S. L. Wiskur, J. F. F. Andersen and E. V. Anslyn, *Angew. Chem., Int. Ed.*, 2002, **41**, 4014; (*g*) M. Komiyama, S. Kina, K. Matsumura, J. Sumaoka, S. Tobey, V. M. Lynch and E. V. Anslyn, *J. Am. Chem. Soc.*, 2002, **124**, 13731; (*h*) K. Worm, F. Chu, K. Matsumoto, M. D. Best, V. Lynch and E. V. Anslyn, *Chem.–Eur. J.*, 2003, **9**, 741; (*i*) V. Jubian, A. Veronese, R. P. Dixon and A. D. Hamilton, *Angew. Chem., Int. Ed. Engl.*, 1995, **34**, 1237; (*j*) S. Liu, Z. Luo and A. D. Hamilton, *Angew. Chem., Int. Ed.*, 1997, **36**, 2678; (*k*) S. Liu and A. D. Hamilton, *Chem. Commun.*, 1999, 587; (*l*) P. Molenveld, J. F. J. Engbersen, H. Kooijman, A. L. Speck and D. N. Reinhoudt, *J. Am. Chem. Soc.*, 1998, **120**, 6726; (*m*) L. Bonfa, M. Gato, F. Mancin, P. Tecilla and U. Tonellato, *Inorg. Chem.*, 2003, **42**, 3943; (*n*) F. Mancin, P. Scrimin, P. Tecilla and U. Tonellato, *Chem. Commun.*, 2005, 2540; (*o*) F. Mancin and P. Tecilla, *New J. Chem.*, 2007, **31**, 800; (*p*) R. Cacciapaglia, A. Casnati, L. Mandolini, D. N. Reinhoudt, R. Salvio, A. Sartori and R. Ungaro, *J. Am. Chem. Soc.*, 2006, **128**, 12322; (*q*) R. Cacciapaglia, A. Casnati, L. Mandolini, A. Peracchi, D. N. Reinhoudt, R. Salvio, A. Sartori and R. Ungaro, *J. Am. Chem. Soc.*, 2007, **129**, 12512.
7 (*a*) S. Takebayashi, M. Ikeda, M. Takeuchi and S. Shinkai, *Chem. Commun.*, 2004, 420; (*b*) A. Ojida, M.-a. Inoue, Y. Mito-oka and I. Hamachi, *J. Am. Chem. Soc.*, 2003, **125**, 10184.
8 (*a*) J. K. Romary, J. D. Barger and J. E. Bunds, *Inorg. Chem.*, 1968, **7**, 1142; (*b*) R. M. Smith and A. E. Martell, *Critical Stability Constants*, Plenum, New York, 1st edn, 1982, vol. 5.
9 (*a*) A. Goller and U. W. Grummt, *Chem. Phys. Lett.*, 2000, **321**, 401; (*b*) Rebek *et al*. have reported a significant reaction rate enhancement in the cyclization of 6,6′-substituents by Ni^{2+} complexation with 2,2′-bipyridine: J. Rebek, Jr., T. Costello and R. Wattley, *J. Am. Chem. Soc.*, 1985, **107**, 7487, see also ref. 1*b*;; (*c*) recently,Lehn and co-workers have utilized a transoid conformation to create supramolecular helices: L. A. Cuccia, J.-M. Lehn, J.-C. Homo and M. Schmutz, *Angew. Chem., Int. Ed.*, 2000, **38**, 233; (*d*) K. M. Gardinier, R. G. Khoury and J.-M. Lehn, *Chem.–Eur. J.*, 2000, **6**, 4124.
10 A. F. Abdel-Magid, K. G. Carson, B. D. Harris, C. A. Maryanoff and R. D. Shah, *J. Org. Chem.*, 1996, **61**, 3849.
11 M. Koyama, K. Takahashi, T.-C. Chou, Z. Darzynkiewicz, J. Kapuscinski, T. R. Kelly and K. A. Watanabe, *J. Med. Chem.*, 1989, **32**, 1594.
12 C. L. Fraser, N. R. Anastasi and J. J. S. Lamba, *J. Org. Chem.*, 1997, **62**, 9314.
13 For **1** with 3.5 equiv. Cu^{2+}, the ratio of $[\mathbf{1}\cdot(Cu^{2+})_3]/[\mathbf{1}_2\cdot(Cu^{2+})_5]/[\mathbf{1}\cdot(Cu^{2+})_2]$ was estimated to be 92/5/3 by the association constants between Cu^{2+} and the Bpy moiety in **1**. The decrease in the k_{obs} value upon addition of more than 3 equiv. Cu^{2+} is-ascribed to the formation of precipitate under these conditions.
14 G. Sprintschnik, H. W. Sprintschnik, P. P. Kirsch and D. G. Whitten, *J. Am. Chem. Soc.*, 1977, **99**, 4947.
15 D. M. Brown and D. A. Usher, *J. Chem. Soc.*, 1965, 6588.